Re-synchronization of Universal Droop Control Distributed Generation Inverter to the Grid

Mohammad Amin
Department of Electric Power Engineering
Norwegian University of Science and Technology
Trondheim-7491, Norway
Email: mohammad.amin@ntnu.no

Qing-Chang Zhong
Dept. of Electrical and Computer Engineering
Illinois Institute of Technology
Chicago, IL 60616, USA
Email: zhongqc@iit.edu

***Abstract*—The distributed generation (DG) inverters can operate in an islanded mode and a grid-connected mode. Under grid fault conditions, the inverter is disconnected from the main grid and operates in the islanded mode. When DG inverters operate in the islanded mode, they often form a microgrid. The phase and magnitude of the microgrid voltage deviate from the main grid. If the microgrid is connected to the main grid under such condition, it results in a transient overcurrent during the reconnection of the microgrid to the main grid. In order to overcome this problem, this paper presents a new re-synchronization method for universal droop control (UDC) DG inverter. Simulation and experimental results are provided to verify the effectiveness of the proposed method. The result shows that the transient overcurrent can be avoided when a UDC DG inverter-based microgrid connects with the main ac grid.**

***Index Terms*—Re-synchronization, microgrid, islanded mode, universal droop control, inverter control, distributed generation.**

I. Introduction

Power electronics inverters are the enabling technology for integrating renewable energy such as wind power, solar power, tidal power to the grid [1]–[5]. They often form microgrids before being connected to the main grid [6]. A simplified structure of such microgrid is shown in Fig. 1. The inverter can be fed by a renewable energy source or battery energy storage system. Both the inverter and local load are connected to the main grid through an active switch S_1. The state of the switch S_1, as well as the operation mode of the inverter, depends upon the state of the main grid. Considering this study case, two operating modes of the inverter system can be achieved. The first operating mode is the grid-connected mode when both switches S_1 and S_2 are on. In this mode, the main objective of the inverter is to export the available power from the renewable source to the grid. Moreover, the inverter supports the grid by contributing to the voltage and frequency regulation [7], [8].

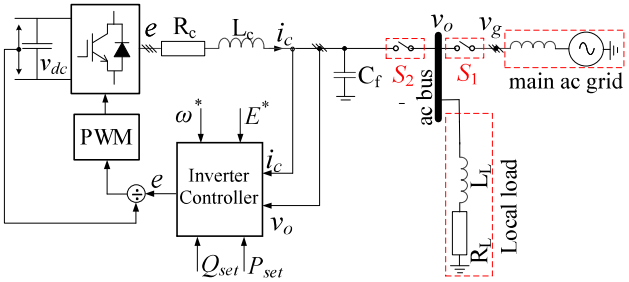

Fig. 1. A grid-connected DG inverter with a local load.

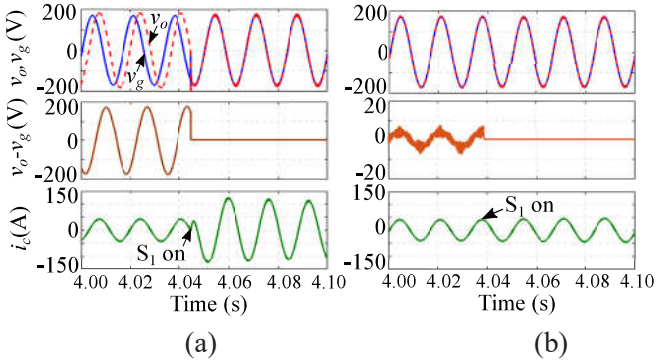

Fig. 2. Grid connection of the inverter, (a) S_1 turned on without re-synchronization resulting in a large inrush current and (b) S_1 turned on after re-synchronization resulting in no inrush current.

The other mode of the operation of the inverter is the islanded mode. Under grid fault conditions, the switch S_1 disconnects the inverter from the main grid when the inverter supplies the power to the local load. Under such condition, the inverter works in the grid forming mode and regulates the voltage and the frequency of the microgrid [9], [10]. When the grid voltage is restored, the magnitude and the phase of the grid voltage may not be the same as the microgrid voltage. If the inverter is connected to

the grid under such condition, it will result in a transient overcurrent that could be harmful to the system. An example of such a condition is presented in Fig. 2. The inverter operates at its rated power. Two scenarios are presented. In the first scenario, the switch S_1 is turned on without performing synchronization. As can be seen, a 3-times of the rated current flows when the switch is turned on. In the second scenario, the switch S_1 is turned on after synchronization resulting in no inrush current when the switch S_1 is turned on. Therefore, before turning on the switch S_1 for connecting the inverter to the grid, it is necessary to re-synchronize the microgrid voltage with the main grid to avoid such high inrush current.

The re-synchronization of a microgrid is usually accomplished by detecting the phase difference between the main grid and the microgrid, where the phase of the voltage is detected using a phase-locked-loop (PLL) [11]–[16]. The PLL presents a proper performance under a balance voltage condition, however, its performance deficits significantly under an unbalanced and distorted condition of the grid voltage. Moreover, its performance is very sensitive to a sudden change of phase of the voltage, even sometimes, it introduces an instability problem in power converters [17]. Therefore, the PLL is less reliable when synchronizing the inverter to the grid. Frequency-locked-loop (FLL) is often used for synchronization purpose [18]. However, the FLL brings a computational complexity in tuning the parameters and is difficult in hardware realization.

Recently, in [19], a universal droop control (UDC) is proposed for grid-connected inverters. An initial synchronization mechanism is embedded with the UDC to form a self-synchronized UDC (SUDC) without a PLL or FLL [20]. The SUDC inverter can automatically synchronize itself with the grid before connection and track the grid frequency after connection. The SUDC inverter operates both the grid-connected mode and the islanded mode. It can switch it's operation mode from the grid-connected mode to the islanded mode, however, it can not switch it's operation mode from the islanded mode to the grid-connected mode due to lack of a re-synchronization mechanism. This paper presents a re-synchronization mechanism for the SUDC inverter. The proposed re-synchronization mechanism allows a change of the SUDC's operation mode from the islanded mode to the grid-connected mode smoothly and vice-versa. Simulation and experimental results are provided to verify the effectiveness of the proposed re-synchronization method. The result shows that the inrush can be avoided when a UDC inverter with a local load connects with the grid.

II. The Proposed Re-synchronization Mechanism for the UDC Inverter

When the grid voltage is restored, the microgrid ac bus voltage v_o deviates from the main grid voltage v_g. The voltage error between the microgrid and the main grid is

$$v_{err} = v_o - v_g. \tag{1}$$

For the purpose of implementing the re-synchronization mechanism, a virtual impedance $sL + R$ is introduced in between the microgrid ac bus and the main grid. In the controller, a virtual current i_r can be generated via passing the voltage error v_{err} through the virtual impedance as

$$i_r = \frac{v_o - v_g}{sL + R}. \tag{2}$$

The real power and the reactive power due to this virtual current i_r can be given by

$$\begin{aligned} P_v &= \left(\frac{V_o V_g}{Z_v}\cos(\theta_o - \theta_g) - \frac{V_o^2}{Z_v}\right)\cos\theta_v \\ &\quad + \frac{V_o V_g}{Z_v}\sin(\theta_o - \theta_g)\sin\theta_v \end{aligned} \tag{3}$$

$$\begin{aligned} Q_v &= \left(\frac{V_o V_g}{Z_v}\cos(\theta_o - \theta_g) - \frac{V_o^2}{Z_v}\right)\sin\theta_v \\ &\quad - \frac{V_o V_g}{Z_v}\sin(\theta_o - \theta_g)\cos\theta_v \end{aligned} \tag{4}$$

where V_o and V_g are the RMS value of the microgrid ac bus voltage and the main grid voltage, respectively, and θ_o and θ_g are their corresponding phase angle, Z_v and θ_v is the magnitude and angle of the virtual impedance. The virtual impedance is usually selected to be either inductive or resistive depending on the control implementation of the inverter. In this study, we have implemented the universal droop controller (UDC) [20], where the impedance of the inverter is assumed to be dominantly resistive. The same assumption is kept for the virtual impedance. Therefore, the virtual impedance is selected to be dominantly resistive, which gives $\theta_v \approx 0$. Hence, the active power and the reactive power resulting from the virtual current can be rewritten as

$$P_v = \frac{V_o}{Z_v}\left(V_g\cos(\theta_o - \theta_g) - V_o\right) \tag{5}$$

$$Q_v = -\frac{V_o V_g}{Z_v}\sin(\theta_o - \theta_g). \tag{6}$$

In the re-synchronization process, the inverter operates in the islanded mode and there is no physical connection between the microgrid and the main grid, as a result, no actual real power and reactive power can be exchanged in between the main grid and the microgrid. Therefore, the current carried by the virtual impedance will be regulated

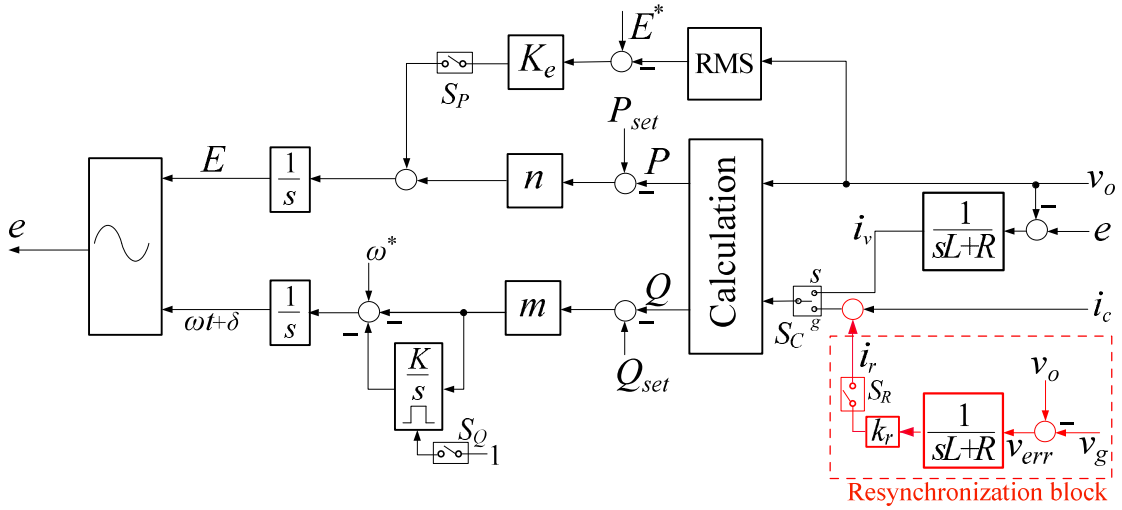

Fig. 3. Self-synchronized universal droop controller with re-synchronization-loop.

to be zero. Both P_v and Q_v will be eventually driven to zero. Eqn. (5) indicates that the virtual power P_v and Q_v can only be zero when

$$V_o = V_g \text{ and } \theta_o = \theta_g. \tag{7}$$

The inverter controller drives the microgrid voltage and frequency in such that it satisfies condition (7). In other words, the inverter voltage v_o is synchronized with the grid voltage v_g. The voltage and phase difference between the inverter voltage and the grid voltage will be zero. Hence, the switch S_1 can be turned ON any time to reconnect the inverter to the grid.

III. Realization of the Re-synchronization with the SUDC

A. Overview of the SUDC inverter

The SUDC is shown in Fig. 3 without the red dashed box. The UDC is proposed as [19]

$$E = \frac{1}{s}\left[n\left(P_{set} - P\right) + S_P K_e\left(E^* - V_o\right)\right] \tag{8}$$

$$\omega = \omega^* - m\left(Q_{set} - Q\right) \tag{9}$$

where E^* is the reference RMS value of the output voltage; ω^* is the rated system frequency; n and m are the droop coefficient; P and Q are the output active and reactive power of the inverter; P_{set} and Q_{set} are the reference active and reactive power of the inverter, respectively; K_e and K are positive gain, and S_P are switching state, 1 for ON and 0 for OFF. The UDC is applicable to inverters with an impedance angle of $-\pi/2$ to $\pi/2$ rad [19].

Before turning on the PWM, the inverter voltage e should be synchronized with the terminal voltage v_o. Therefore, an initial self-synchronization mechanism is proposed in [20]. In order to achieve that, the switch S_C in Fig. 3 is put at the position "s" and the power reference values P_{set} and Q_{set} are set zero, respectively. A virtual current is generated via passing the voltage error $e - v_o$ through the virtual impedance $sL + R$ as shown in Fig. 3 for the initial synchronization. More detail on this self-synchronization mechanism can be found in [20].

B. Re-synchronization Process

When the grid voltage is restored, the magnitude difference between the main grid voltage and the microgrid voltage may not be that significant. The transient overcurrent is mainly due to the phase difference between these two voltages [18]. The magnitude of the virtual current can be as high as two times of the rated current depending on the phase difference. Such a high transient current may introduce an instability problem to the controller. Therefore, a positive constant k_r is introduced, which value can be kept in between $0 < k_1 \leq 0.5$, in order to limit the virtual current. Moreover, an additional switch S_R is added with the SUDC for embedding the re-synchronization mechanism. Fig. 3 depicts the SUDC with the re-synchronization block in the dashed box. When the switch S_R is ON, the total current to the controller will be the sum of the inverter current i_c plus the virtual current i_r. The actual power send by the inverter is calculated using the ac bus voltage v_o and inverter current i_c as

$$P + jQ = v_o i_c^*. \tag{10}$$

TABLE I
PARAMETERS OF THE SIMULATED SYSTEM.

Parameters	Values
Rated Power	20 kVA
Rated phase voltage (RMS), V_o	120 V
Rated dc voltage, V_{dc}	400 V
Rated frequency, f	60 Hz
Inverter series inductance, L_c	0.25 pu
Inverter series resistance, R_c	0.05 pu
Filter capacitance, C_f	0.018 pu

Hence, the total active power and the reactive power are

$$P_t = P + P_v \tag{11}$$

$$Q_t = Q + Q_v. \tag{12}$$

During the re-synchronization process, the active power P and reactive Q are the actual real power and the reactive power drawn by the connected load. P_v and Q_v are the active and reactive power introduced by the virtual current. Since no real power or reactive power will be exchanged in between the main grid and the microgrid at the steady-state, the current i_r carried by the virtual impedance is regulated to be zero as a result both P_v and Q_v will eventually drive to zero. P_v and Q_v become zero when $V_o = V_g$ and $\theta_o = \theta_g$, meaning that the inverter voltage v_o is synchronized with the grid voltage v_g. Hence, the switch S_1 can be turned on any time to reconnect the inverter to the grid.

IV. Simulation and Experimental Validation

In order to verify the effectiveness of the proposed re-synchronization method, simulation and experiments are carried out. The results have described in the following.

A. Simulation

The system shown in Fig. 1 has been implemented in Matlab/Simulink association with SimPower System with a switching model of the inverter. The simulated system parameters are given in Table I. The local load is 10 kW. The positive gain k_r is set to 0.5. Fig. 4 shows the micro-grid ac bus voltages, grid voltages, voltages error between the microgrid and main grid voltage, inverter currents, active power, and reactive power from the simulation. The simulation scenario is divided into four parts: i) inverter OFF; ii) grid-connected operation, iii) islanded operation and iv) grid-reconnected operation. This paper focuses on the fourth part of this simulation, i.e. this paper proposes a mechanism for reconnection of the SUDC inverter to the main ac grid. Initially, the inverter operates in the self-synchronization mode and the PWM of the inverter is off.

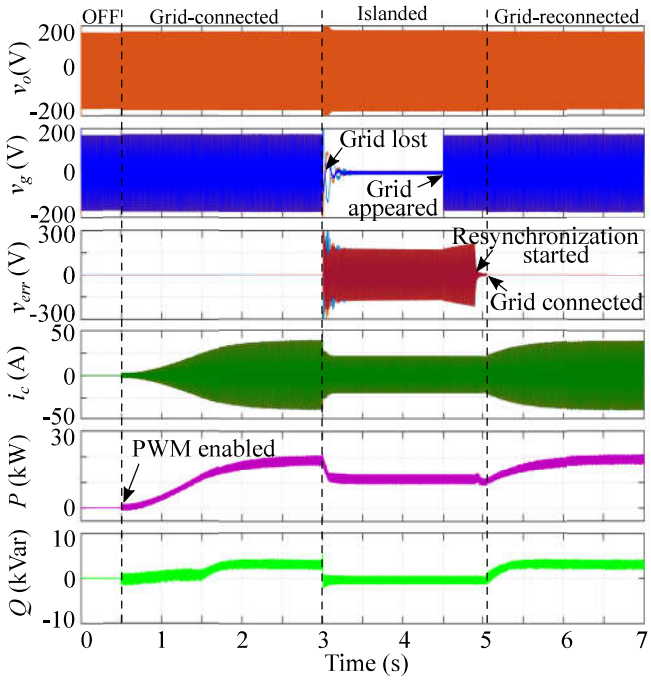

Fig. 4. Simulation: Initially, the inverter is OFF. The PWM is enabled at 0.5 s. The grid is lost at 3 s and restored at 4.5 s. The re-synchronization started at 4.90 s and the island operation mode changed to the grid-connected mode at 5.05 s.

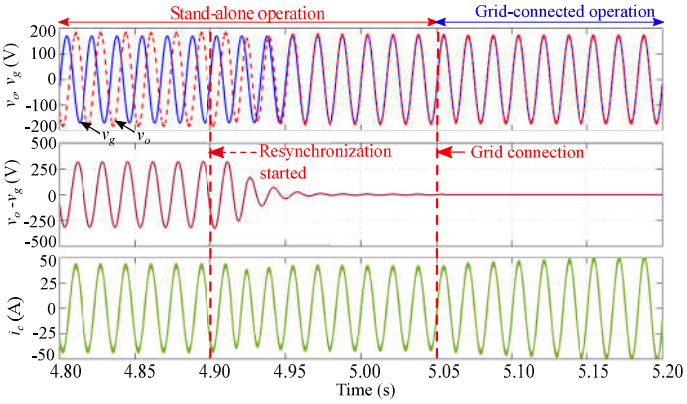

Fig. 5. Simulation of re-synchronization process of the UDC DG inverter: at $t = 4.90$ s, the switch S_R is on to start the re-synchronization process and at $t = 5.05$ s, the switch S_1 is on for grid connection.

At 0.50 s, the inverter's PWM is enabled and the inverter starts sending power according to its set power, $P_{set} = 20$ kW. At 3.0 s, the main grid is lost and the active switch S_1 is opened. The local load is powered by the inverter. At 4.50 s, the main grid appears. As can be seen, there is a large voltage error $v_{err} = v_o - v_g$ when the main grid is lost as well as when the grid appears. The phase-A ac bus voltage, grid voltage, voltage error and inverter

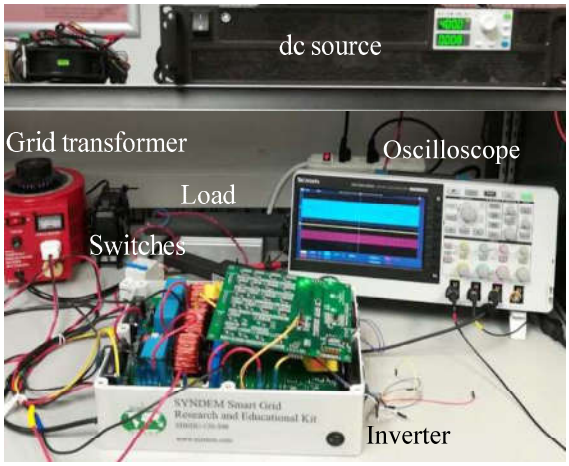

Fig. 6. Experimental setup.

TABLE II
PARAMETERS OF THE EXPERIMENTAL SYSTEM.

Parameters	Values
Rated voltage (L-L, RMS), V_o	208 V
Rated dc voltage,V_{dc}	400 V
Rated frequency, f	60 Hz
Inverter series inductance, L_c	2.2 mH
Filter capacitance, C_f	22 μF

current are shown in Fig. 5. The voltage magnitude and phase are different which result in a high voltage error v_{err}. At 4.90 s, the switch S_R is turned on to start the re-synchronization. The microgrid ac bus voltage is able to track the main grid voltage within a few cycles and the voltage error v_{err} becomes nearly zero, which means the microgrid voltage is synchronized with the main grid. Since the voltage is synchronized, the active switch S_1 can be turned on to connect the inverter to the main grid. At 5.05 s, the switch S_1 is turned on to connect the inverter to the main grid. The bottom plot of Fig. 5 shows the current of the inverter. Since the voltages are synchronized, there is no transient overcurrent. The islanded mode has changed to the grid-connected mode smoothly.

B. Experiment

After validating the proposed method in the simulation, an experiment is carried. The SUDC together with the re-synchronization mechanism is implemented on a TMS320F28335 DSP with the sampling frequency of 10 kHz. Some signals are sent out via a DAC chip and recorded with an oscilloscope. A photo of the experimental setup based on a SYNDEM smart grid research and educational kit is shown in Fig. 6. The parameters of the inverter system are given in Table II. A 300-W load is connected to the ac bus of the microgrid. Initially, the inverter operates in the stand-alone mode and supplies power to the local load, while maintaining the rated frequency and voltage. The experimental result is shown in Fig. 7. The initial synchronization and the grid lost is not shown in the experimental result. At 0.8 s, the switch S_R is turned on to start the re-synchronization. A zoom view of the re-synchronization process is shown in the top right plot. As can be seen, before starting the synchronization process, there is a large phase difference between the microgrid voltage and the main ac grid voltage. When the switch S_R is on, the phase difference starts reducing and after some cycles v_{err} becomes zero, which means, the microgrid voltage synchronizes with the main grid voltage. When the synchronization is complete, the switch S_1 can be turned on anytime to connect the microgrid with the main ac grid. Here the switch S_1 is turned on at 2.56 s to connect the microgrid to the main grid. A zoom view of the grid connection is also shown in the bottom right of Fig. 7. The microgrid smoothly reconnects to the main grid without any transient overcurrent.

V. CONCLUSION

This paper presents a new re-synchronization mechanism for the UDC inverter. The proposed re-synchronization mechanism allows a change of the UDC's operation mode from the islanded mode to the grid-connected mode smoothly. Simulation and experimental results are provided to verify the effectiveness of the proposed re-synchronization method. The result shows that the transient overcurrent can be avoided when a microgrid connects with the main grid. The proposed re-synchronization mechanism for the UDC can be deployed in large microgrids to achieve a seamless connection/reconnection of microgrids to the main grid.

REFERENCES

[1] F. Blaabjerg, F. Iov, R. Teodorescu, and Z. Chen, "Power electronics in renewable energy systems," in *Proc. of the 12th International Power Electronics and Motion Control Conference (EPE-PEMC)*, 2006, pp. 1–17.

[2] F. Blaabjerg, M. Liserre, and K. Ma, "Power electronics converters for wind turbine systems," *IEEE Trans. Ind. Appl.*, vol. 48, no. 2, pp. 708–719, March 2012.

[3] F. Blaabjerg and K. Ma, "Wind energy systems," *Proc. IEEE*, vol. 105, no. 11, pp. 2116–2131, Nov 2017.

[4] J. Carrasco, L. Franquelo, J. Bialasiewicz, E. Galvan, R. Portillo-Guisado, M. Prats, J. Leon, and N. Moreno-Alfonso, "Power-electronic systems for the grid integration of renewable energy sources: A survey," *IEEE Trans. Ind. Electron.*, vol. 53, no. 4, pp. 1002–1016, Jun. 2006.

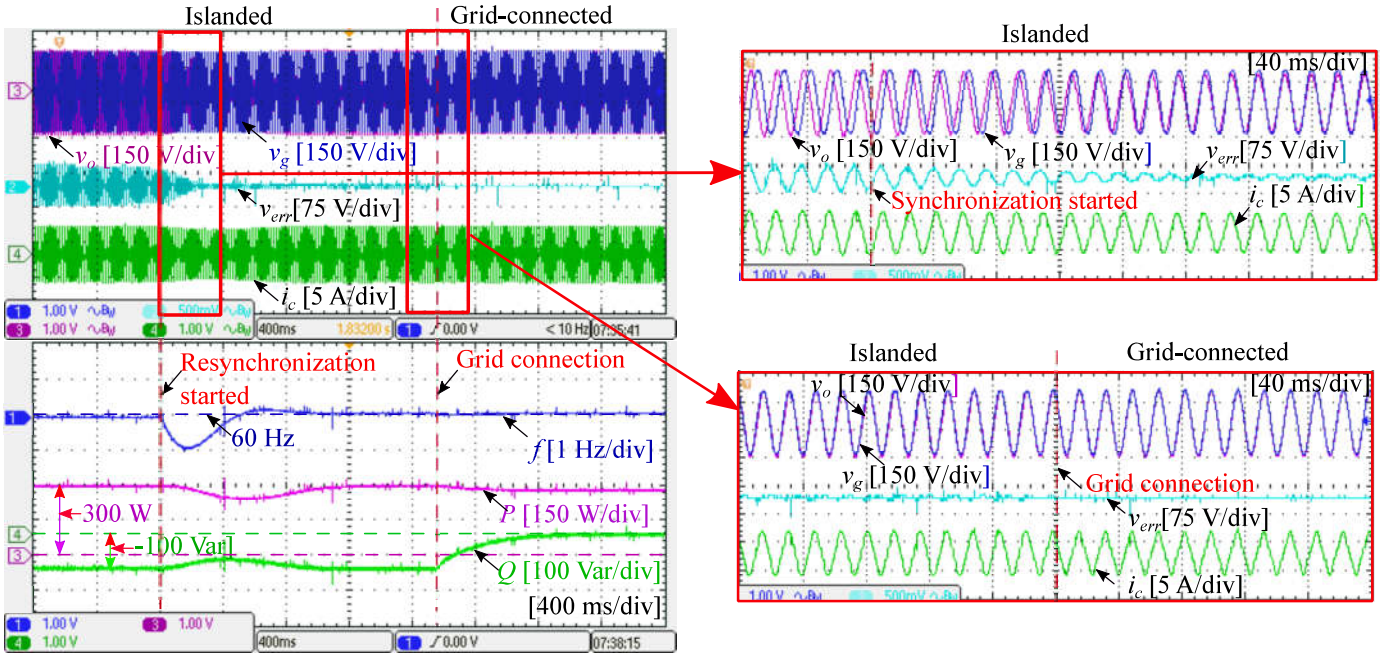

Fig. 7. Experiment of the re-synchronization process of the DG inverter with a local load.

[5] L. Wang, Q. H. Wu, and W. Tang, "Novel cascaded switched-diode multilevel inverter for renewable energy integration," *IEEE Trans. Energy Convers.*, vol. 32, no. 4, pp. 1574–1582, Dec 2017.

[6] E. Serban and H. Serban, "A control strategy for a distributed power generation microgrid application with voltage and current controlled source converter," *IEEE Trans. Power Electron.*, vol. 25, no. 12, pp. 3015–3025, Aug. 2010.

[7] Q.-C. Zhong, "Power electronics-enabled autonomous power systems: Architecture and technical routes," *IEEE Trans. Ind. Electron.*, vol. 64, no. 7, pp. 5907–5918, Jul. 2017.

[8] J. C. Vasquez, R. A. Mastromauro, J. M. Guerrero, and M. Liserre, "Voltage support provided by a droop-controlled multifunctional inverter," *IEEE Trans. Ind. Electron.*, vol. 56, no. 11, pp. 4510–4519, Nov 2009.

[9] R. M. Kamel, A. Chaouachi, and K. Nagasaka, "Three control strategies to improve the microgrid transient dynamic response during isolated mode: A comparative study," *IEEE Trans. Ind. Electron.*, vol. 60, no. 4, pp. 1314–1322, April 2013.

[10] J. Rocabert, A. Luna, F. Blaabjerg, and P. Rodríguez, "Control of power converters in ac microgrids," *IEEE Trans. Power Electron.*, vol. 27, no. 11, pp. 4734–4749, Nov 2012.

[11] H. Kim, T. Yu, and S. Choi, "Indirect current control algorithm for utility interactive inverters in distributed generation systems," *IEEE Trans. Power Electron.*, vol. 23, no. 3, pp. 1342–1347, May 2008.

[12] M. Ramezani, S. Li, F. Musavi, and S. Golestan, "Seamless transition of synchronous inverters using synchronizing virtual torque and flux linkage," *IEEE Trans. Ind. Electron.*, pp. 1–1, 2019.

[13] C.-L. Chen, Y. Wang, J.-S. Lai, Y.-S. Lee, and D. Martin, "Design of parallel inverters for smooth mode transfer microgrid applications," *IEEE Trans. Power Electron.*, vol. 25, no. 1, pp. 6–15, Feb. 2010.

[14] J. Vasquez, J. Guerrero, A. Luna, P. Rodriguez, and R. Teodorescu, "Adaptive droop control applied to voltage-source inverters operating in grid-connected and islanded modes," *IEEE Trans. Ind. Electron.*, vol. 56, no. 10, pp. 4088–4096, Oct. 2009.

[15] M. Arafat, A. Elrayyah, and Y. Sozer, "An effective smooth transition control strategy using droop-based synchronization for parallel inverters," *IEEE Trans. Ind. Appl.*, vol. 51, no. 3, pp. 2443–2454, May 2015.

[16] D. S. Ochs, B. Mirafzal, and P. Sotoodeh, "A method of seamless transitions between grid-tied and stand-alone modes of operation for utility-interactive three-phase inverters," *IEEE Trans. Ind. Appl.*, vol. 50, no. 3, pp. 1934–1941, May 2014.

[17] B. Wen, D. Dong, D. Boroyevich, R. Burgos, P. Mattavelli, and Z. Shen, "Impedance-based analysis of grid-synchronization stability for three-phase paralleled converters," *IEEE Trans. Power Electron.*, vol. 31, no. 1, pp. 26–38, Jan 2016.

[18] J. Rocabert, G. M. S. Azevedo, A. Luna, J. M. Guerrero, J. I. Candela, and P. Rodríguez, "Intelligent connection agent for three-phase grid-connected microgrids," *IEEE Trans. Power Electron.*, vol. 26, no. 10, pp. 2993–3005, Oct 2011.

[19] Q.-C. Zhong and Y. Zeng, "Universal droop control of inverters with different types of output impedance," *IEEE Access*, vol. 4, pp. 702–712, Jan. 2016.

[20] Q.-C. Zhong, W. L. Ming, and Y. Zeng, "Self-synchronized universal droop controller," *IEEE Access*, vol. 4, pp. 7145–7153, Oct. 2016.